

Can pre-ozonation be combined with gravity-driven membrane filtration to treat shale gas wastewater?

Original

Can pre-ozonation be combined with gravity-driven membrane filtration to treat shale gas wastewater? / Tang, Peng; Shi, Mengchao; Li, Xin; Zhang, Yongli; Lin, Dong; Li, Tong; Zhang, Weiming; Tiraferri, Alberto; Liu, Baicang. - In: SCIENCE OF THE TOTAL ENVIRONMENT. - ISSN 0048-9697. - 797:(2021), p. 149181.
[10.1016/j.scitotenv.2021.149181]

Availability:

This version is available at: 11583/2915978 since: 2021-07-30T11:18:15Z

Publisher:

Elsevier B.V.

Published

DOI:10.1016/j.scitotenv.2021.149181

Terms of use:

This article is made available under terms and conditions as specified in the corresponding bibliographic description in the repository

Publisher copyright

(Article begins on next page)

1 Can pre-ozonation be combined with gravity
2 driven membrane filtration to treat shale gas
3 wastewater?

4 *Peng Tang*^{a,b}, *Mengchao Shi*^{a,b}, *Xin Li*^{a,b}, *Yongli Zhang*^a, *Dong Lin*^c, *Tong Li*
5 *d,**, *Weiming Zhang*^e, *Alberto Tiraferri*^f, *Baicang Liu*^{a,b,**}

6 ^a Key Laboratory of Deep Earth Science and Engineering (Ministry of Education),
7 College of Architecture and Environment, Institute of New Energy and Low-Carbon
8 Technology, Institute for Disaster Management and Reconstruction, Sichuan University,
9 Chengdu, Sichuan 610207, PR China

10 ^b Yibin Institute of Industrial Technology, Sichuan University, Yibin Park, Section 2,
11 Lingang Ave., Cuiping District, Yibin, Sichuan 644000, PR China

12 ^c PetroChina Southwest Oil and Gas field Company, No.5 Fuqing Rd., Chengdu,
13 Sichuan 610051, PR China

14 ^d School of Energy and Environmental Engineering, University of Science &
15 Technology Beijing, Beijing, 100083, PR China

16 ^e State Key Laboratory of Pollution Control and Resource Reuse, School of the
17 Environment, Nanjing University, Nanjing 210023, PR China

18 ^f Department of Environment, Land and Infrastructure Engineering, Politecnico di
19 Torino, Corso Duca degli Abruzzi 24, 10129 Turin, Italy

20

21 **Abstract:** Low-cost gravity-driven membrane (GDM) filtration combined with
22 appropriate pre-treatment processes has major potential to efficiently manage shale
23 gas wastewater (SGW). In this work, the feasibility of combining low dosage
24 pre-ozonation with the GDM process was evaluated in the treatment of SGW. The
25 results showed that pre-ozonation significantly increased the stable flux (372%) of
26 GDM filtration, while slightly deteriorating the quality of the effluent water in terms
27 of organic content (-14%). These results were mainly attributed to the conversion of
28 macromolecular organics to low-molecular weight fractions by pre-ozonation.
29 Interestingly, pre-ozonation markedly increased the flux (198%) in the first month of
30 operation also for a GDM process that comprised the addition of GAC (GGDM).
31 Nevertheless, the flux of O₃-GGDM systems dropped sharply around the 25th day of
32 operation, which might be due to the rapid accumulation of pollutants in the high flux
33 stage and the formation of a dense fouling layer. Pre-ozonation remarkably influenced
34 the microbial community structure and O₃-GDM systems were characterized by
35 distinct core microorganisms, which could degrade specific organics in SGW.
36 Furthermore, O₃-GDM outperformed simple GDM as a pretreatment for RO. These
37 findings can provide valuable references for combining oxidation technologies with
38 the GDM process in treating refractory wastewater.

39

40 **Keywords:** Shale gas wastewater; Pre-ozonation; Gravity driven membrane filtration;
41 Mechanism

42 **1. Introduction**

43 Horizontal drilling and hydraulic fracturing technologies are applied to overcome
44 the challenge of shale gas extraction. Nevertheless, a large amount (~5200-25,870 m³
45 per well) of shale gas wastewater (SGW) is produced during hydraulic fracturing
46 (Kondash and Vengosh, 2015). SGW is typically characterized by high salinity and
47 high concentrations of toxic metals and organics (Butkovskyi et al., 2017). If not
48 treated properly, its discharge would seriously threaten the water environment and
49 human health. At present, hybrid membrane technologies are regarded as suitable and
50 effective means to treat SGW (Tong et al., 2019). Specifically, low-pressure
51 membrane processes, such as ultrafiltration (UF), are investigated and implemented as
52 pretreatment steps for the subsequent desalination (Chang et al., 2019b; Guo et al.,
53 2018; Miller et al., 2013). However, operational problems associated with membrane
54 fouling seriously reduce the efficacy and economy of UF (Shang et al., 2019; Tang
55 et al., 2020).

56 Gravity driven membrane filtration (GDM), a recently developed membrane
57 technology, has been proposed to replace traditional UF in the pretreatment of SGW
58 (Chang et al., 2019a). The main rationale is that GDM filtration does not need
59 cleaning and can obtain a stable flux driven solely by gravity with the advantages of
60 simple operation, low cost, and low energy consumption (Pronk et al., 2019). The
61 feasibility of the GDM process as a pretreatment option for SGW desalination was
62 verified in a number of research efforts (Chang et al., 2019a; Tang et al., 2021a).

63 While underlining the potential of GDM filtration, these studies highlighted the
64 current need for significant improvements in stable flux values and contaminant
65 removal rates of this technology (Chang et al., 2019a; Tang et al., 2021a).

66 Some processes, including adsorption, aeration, and coagulation were
67 successfully combined with GDM to the purpose of improving its performance (Ding
68 et al., 2016; Lee et al., 2021; Tang et al., 2021c). As a strong oxidant, ozone was
69 shown to effectively alleviate membrane fouling when used as a pretreatment process
70 for UF and for membrane bioreactors (MBR) (Sathya et al., 2019; Tang et al., 2020;
71 Wang et al., 2017; Zhang et al., 2020), owing to a reduction of organics molecular
72 size, an enhancement of foulants hydrophilicity, and a decrease of biofouling (Wang
73 et al., 2017). Therefore, we hypothesize that pre-ozonation should also effectively
74 increase the performance of GDM filtration. Generally, it is not recommended to
75 combine pre-ozonation with GDM in the treatment of drinking water, because
76 pre-ozonation has the risk of deteriorating water quality and may produce toxic
77 by-products (Tang et al., 2021b). On the other hand, these issues should not impact
78 the application of GDM filtration to treat wastewater, because this technology would
79 not act as a final polishing step, but instead as pretreatment for subsequent tertiary or
80 desalination processes. The high potential of applying advanced oxidation in the
81 specific treatment of SWG and other producted waters has been recently highlighted
82 and it is of great significance to study synergy of ozonation and GDM filtration, two
83 of the most promising processes for efficient SGW management.

84 Therefore, in this study pre-ozonation is investigated in combination with GDM
85 filtration to treat SGW with the aim of increasing stable flux and contaminant removal
86 values in GDM, and improving the quality of the final desalinated effluent. Six GDM
87 systems are examined to understand the effect of pre-ozonation with low ozone
88 dosage on the performance of GDM systems with and without the presence of an
89 additional treatment step through activated carbon adsorption. The integration
90 between pre-ozonation and GDM filtration is thus discussed, also in the light of the
91 effect on microbial communities that drive membrane fouling and organics removal
92 and biodegradation within the GDM unit.

93

94 **2. Materials and methods**

95 **2.1 Water samples and water quality analysis**

96 SGW samples were collected from the Weiyuan shale gas play (Sichuan Basin,
97 China). The water quality parameters of the SGW are summarized in [Table 1](#). The
98 analytical methods for the determination of turbidity, dissolved organic carbon (DOC),
99 UV₂₅₄, fluorescent organics, and total dissolved solid (TDS) can be found in [Text S1](#)
100 of the Supporting Information (SI) and in our previous study (Tang et al., 2020).

101 **Table 1.** Water quality characteristics of the raw water and the raw water treated by O₃
102 at different dosages.

Parameter	Raw water	Raw water treated by O ₃		
		20 mg/L	40 mg/L	80 mg/L
DOC (mg/L)	17.48	17.91	18.95	18.54

UV ₂₅₄ (cm ⁻¹)	0.095	0.097	0.100	0.098
Turbidity (NTU)	8.2	7.7	7.2	9.6
TDS (g/L)	19.85	20.14	20.71	19.86

103 2.2 Experimental setups and procedures

104 The schematic diagrams and the parameters of the six GDM systems utilized in
105 this work are shown in Fig. S1 and Table 2, respectively. The systems were operated in
106 parallel at room temperature (10-26 °C, Fig. S2) with a hydrostatic pressure of 70 mbar
107 as driving force. The characteristics of the poly(vinylidene fluoride) hollow fiber UF
108 membranes (Litree Purifying Technology Co., Ltd., China) with an effective membrane
109 area of 10 cm² employed in this study can be found in a previous report (Chang et al.,
110 2019a). The systems ran continuously for 90 days, and the flux was monitored
111 through the electronic balance.

112 The system referred to as GDM1 treated raw water without any pre-treatment
113 and represented the control unit. On the other hand, the feed water of four of the six
114 GDM systems (namely, GDM-3, 4, 5, 6) was raw water treated by O₃ at different
115 dosages. Low ozone dosages (20-80 mg/L) were applied and the detailed description
116 of the pre-ozonation process can be found in our previous work (Tang et al., 2020).
117 Before the subsequent GDM filtration, the residual ozone in water was quenched by
118 heating the ozonated effluent at 50 °C for 30 min.

119 Granular activated carbon (GAC, CPG LF 12, Calgon Carbon Co., Ltd., USA)
120 adsorption was included in four of the six GDM systems, specifically, GDM-2, 3, 5, 6.
121 The four systems comprising adsorption are referred to as GGDM units. The GAC

122 was cleaned with deionized water and dried before use. A dosage of 4 g was used to
 123 pre-treat the influent water to the GDM system, a much smaller quantity than that
 124 used in our previous study (Tang et al., 2021a), to slightly reduce the adsorption effect
 125 and highlight the effect of microbial degradation in the membrane reactor.

126 Reverse osmosis (RO) filtration experiments were carried out to verify the effect
 127 of different GDM pre-treatment systems on the desalination performance. The RO
 128 process was operated at a constant applied pressure of 5.5 MPa (55 bar) with 50%
 129 recovery. The RO setup and membrane are described in detail in our previous work
 130 (Tang et al., 2020).

131 **Table 2.** The parameters of six GDM systems.

No.	Aeration	The addition of GAC	Pre-ozonation
GDM1 (GDM)	10 ml/min	-	-
GDM2 (GGDM)	10 ml/min	4 g	-
GDM3 (O ₃ ²⁰ -GGDM)	10 ml/min	4 g	20 mg/L O ₃
GDM4 (O ₃ ⁴⁰ -GDM)	10 ml/min	-	40 mg/L O ₃
GDM5 (O ₃ ⁴⁰ -GGDM)	10 ml/min	4 g	40 mg/L O ₃
GDM6 (O ₃ ⁸⁰ -GGDM)	10 ml/min	4 g	80 mg/L O ₃

132 2.3 Analysis of the membrane fouling layers

133 The measurement and calculation methods of hydraulic resistance of the
 134 membrane fouling layers, namely, the reversible resistance (R_{re}) and the irreversible
 135 resistance (R_{ir}), were identical to our previous study (Chang et al., 2019a). The pure
 136 water contact angles and Fourier transform infrared (FTIR) spectra of membrane
 137 fouling layers were measured with a KRÜSS DSA 25S instrument (KRÜSS GmbH,
 138 Germany) and with an attenuated total reflectance FTIR spectrometer (Nicolet IS 20,

139 Thermo Fisher Scientific Inc., USA), respectively. The surface and the cross-section
140 of the fouled membrane samples, as well as the thickness of membrane fouling layers,
141 were observed and measured by scanning electron microscopy (SEM) (FE-SEM,
142 Regulus-8230, Hitachi, Japan). The surface roughness of the fouled UF membrane
143 samples was determined with atomic force microscopy (AFM, Icon, Bruker,
144 Germany). The extracellular polymer substances (EPS) extraction was conducted
145 using a heating and sonication method and the EPS measuring protocol can be found
146 in our recent studies (Tang et al., 2021d). The fluorescent compounds comprised in
147 the EPS matrix were measured by fluorescence excitation-emission (EEM) (F7000,
148 Hitachi, Japan)

149 **2.4 Microbial diversity analysis**

150 The variation of the microbial community and the dominant functional
151 microorganisms were analyzed through microbial diversity sequencing of the raw
152 water and membrane fouling layers. The amplified primer sets of 16S rRNA genes for
153 bacteria was 338F/806R. Details about microbial diversity sequencing and analysis
154 are presented in [Text S2](#) of the SI and in our previous study (Tang et al., 2021a).

155 **3. Results and discussion**

156 **3.1 Permeate flux and organic matter removal performance**

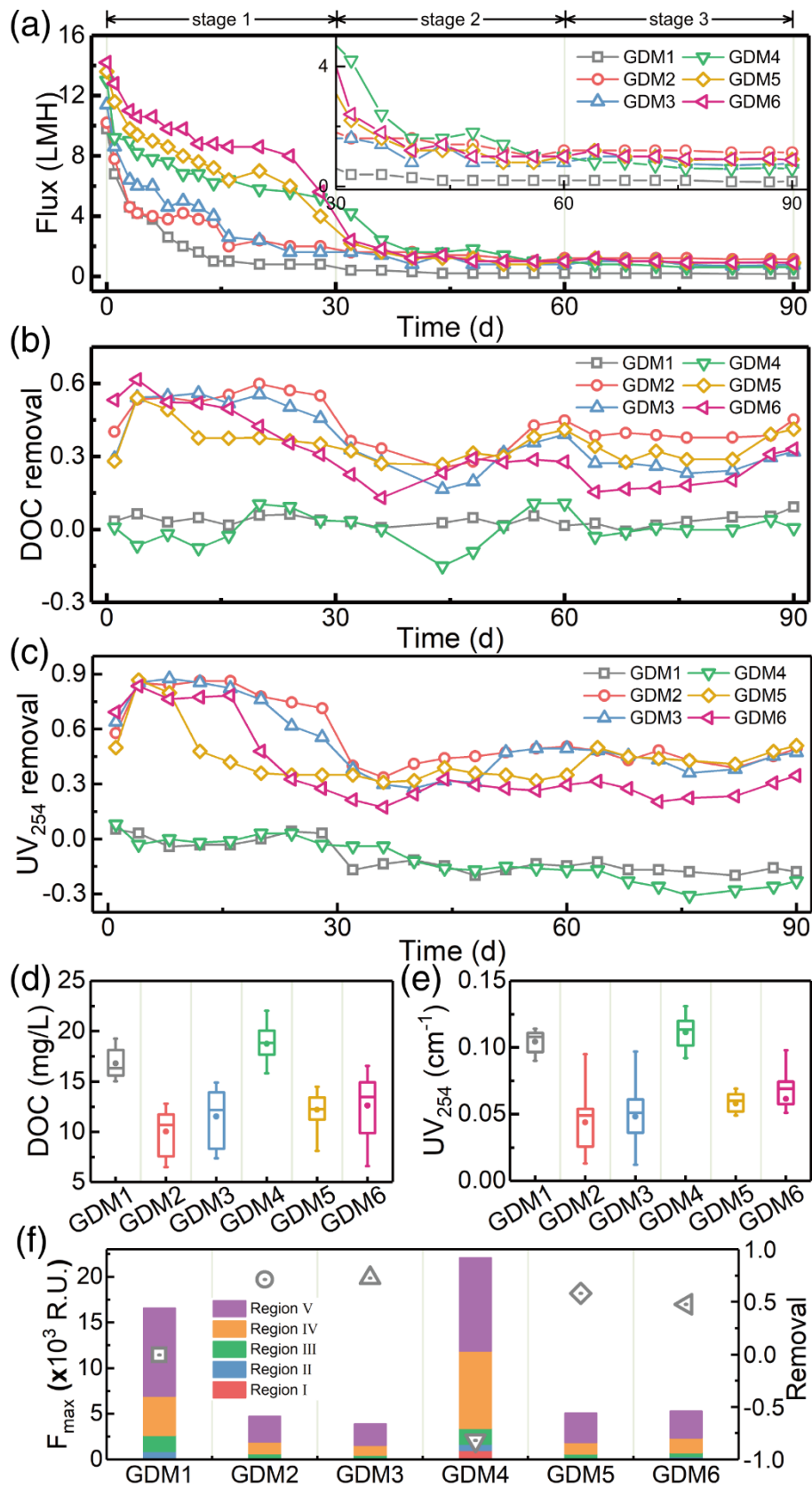
157 The hypothesis of this study is that pre-ozonation performance should influence
158 the behavior of the subsequent GDM filtrations, with possibly higher productivity
159 achievable in the membrane step. As presented in [Table 1](#), the DOC and UV₂₅₄

160 parameters in the raw stream did not decrease upon oxidation, most likely due to the
161 competing effect of mineralization and solubilization of organics (Tang et al., 2021b).
162 Our previous research showed that pre-ozonation mainly changed the organic
163 composition and characteristics of SGW, rather than translating into mineralization of
164 compounds (Tang et al., 2020; Tang et al., 2021b). For example, pre-oxidation
165 significantly improved the biodegradability of SGW (Liu et al., 2018; Tang et al.,
166 2020). The composition and relative content of fluorescent organic matter components
167 in SGW are shown in Fig. S3. The soluble microbial by-product-like matters (region
168 IV) and humic acid-like matters (region V) were the dominant fluorescent organic
169 components in SGW: 3.1%-38.6% of fluorescent organic components were removed
170 by O₃.

171 The flux profiles measured in the six GDM systems are presented in Fig. 1a and
172 analyzed in the light of the pre-oxidation results. The flux trends can be divided into
173 three stages. During the initial filtration stage (stage 1, 0-30 days), a monotonic
174 decline of flux occurred in all the units. However, the flux of GDM systems treating
175 pre-ozonized SGW dropped very slowly and was significantly higher than that of the
176 control GDM system and of the GGDM system without pre-oxidation (GDM2).
177 Specifically, the average flux in the O₃⁴⁰-GDM system was 2.8 times that of GDM
178 and 2.0 times that of GGDM. This result may be attributed to the degradation of
179 macromolecular organic compounds by O₃ into low molecular-weight and more
180 hydrophilic molecules that take more time to deposit on the membrane surface (Tang

181 et al., 2020). However, on the 25th day of operation, the fluxes of O₃-GDM systems
182 also dropped sharply and this phenomenon may be due to the rapid accumulation of
183 pollutants due to the relatively high flux upon the formation of a more homogeneous
184 coating layer at this point of the experiment.

185 Later, the fluxes in the systems continually decreased (second stage, 30-60 days),
186 and ultimately tended to converge to roughly the same steady value (third stage, 60-90
187 days), due to the formation of stable fouling layers on the membrane surfaces. The
188 final stable flux values in the GDM, GGDM, O₃²⁰-GGDM, O₃⁴⁰-GDM, O₃⁴⁰-GGDM,
189 and O₃⁸⁰-GGDM units were 0.18, 1.17, 0.85, 0.67, 0.97, and 0.98 L m⁻²h⁻¹ (LMH),
190 respectively. These results suggest that pre-treatment significantly increased the
191 productivity of the GDM filtration and that: (i) the productivity increased non-linearly
192 but monotonically with ozone dosage; (ii) GAC adsorption significantly helped
193 increasing the GDM flux.



194

195 Fig. 1. (a) Flux profile; (b) DOC removal; and (c) UV₂₅₄ removal measured in the six

196 GDM systems. Values of (d) DOC, (e) UV₂₅₄ in the six effluents. (f) Removal rate and

197 content of fluorescent organics in the effluent of the six systems. GDM1, GDM2,
198 GDM3, GDM4, GDM5, and GDM6 represent control GDM, GGDM, O₃²⁰-GGDM,
199 O₃⁴⁰-GDM, O₃⁴⁰-GGDM, and O₃⁸⁰-GGDM units, respectively.

200

201 [Fig. 1b](#) and [Fig. 1c](#) present the variation of DOC removal and UV₂₅₄ removal
202 rates in the six GDM systems. This rate decreased firstly, then increased, and gradually
203 stabilized. The gradual decrease of GAC adsorption sites is considered to be the main
204 reason for the decline of removal rate in the initial stage; note that the two systems that
205 did not comprise an adsorption process had near zero organics removal in the beginin of
206 the experiments. On the other hand, the increase in removal rate in the second part of
207 the tests may be attributed to the enhancement of microbial degradation and the
208 formation of denser membrane fouling layers (Tang et al., 2021c; Tang et al., 2021d).
209 Instead, the control GDM system and the O₃⁴⁰-GDM system (no GAC adsorption)
210 showed no or decreasing removal rates of organics components, which reached
211 netagive values for UV₂₅₄ compounds.

212 Overall, these observations also support the conclusion that O₃ degraded
213 macromolecular organics into low molecular weight fractions which, when not
214 pre-adsorbed, could directly and more easily pass through into the permeate or
215 undergo biodegradation within the fouling layers, thus further enhancing the passage
216 through the membrane pores. [Fig. 1f](#) presents the composition and the relative content
217 of fluorescent organic compounds in the effluent of the six GDM systems. The four

218 GGDM systems were associated with fluorescent organic compounds (47.6-72.8%).
219 However, the removal rate of fluorescent organic compounds, indicative of soluble
220 microbial by-product-like matters, was negative in the O₃⁴⁰-GDM system. A factor
221 that should also be considered when analyzing removal results is the phenomenon of
222 concentration (Tang et al., 2021a). Since our GDM systems were based on dead-end
223 filtration, contaminants would be concentrated in the reactor and this concentration
224 would be more important for systems associated with higher flux values. We assessed
225 the DOC value in the GDM reactors. (Fig. 1d and Fig. 1e): adsorption effectively
226 reduced the amount of organics in the feed streams to the membranes, and this
227 amount was the highest in the O₃⁴⁰-GDM system, thus also contributing to a more
228 challenging separation and overall negative values of organics removal. Not
229 surprisingly, the higher the productivity of the systems the larger was the observed
230 DOC concentration.

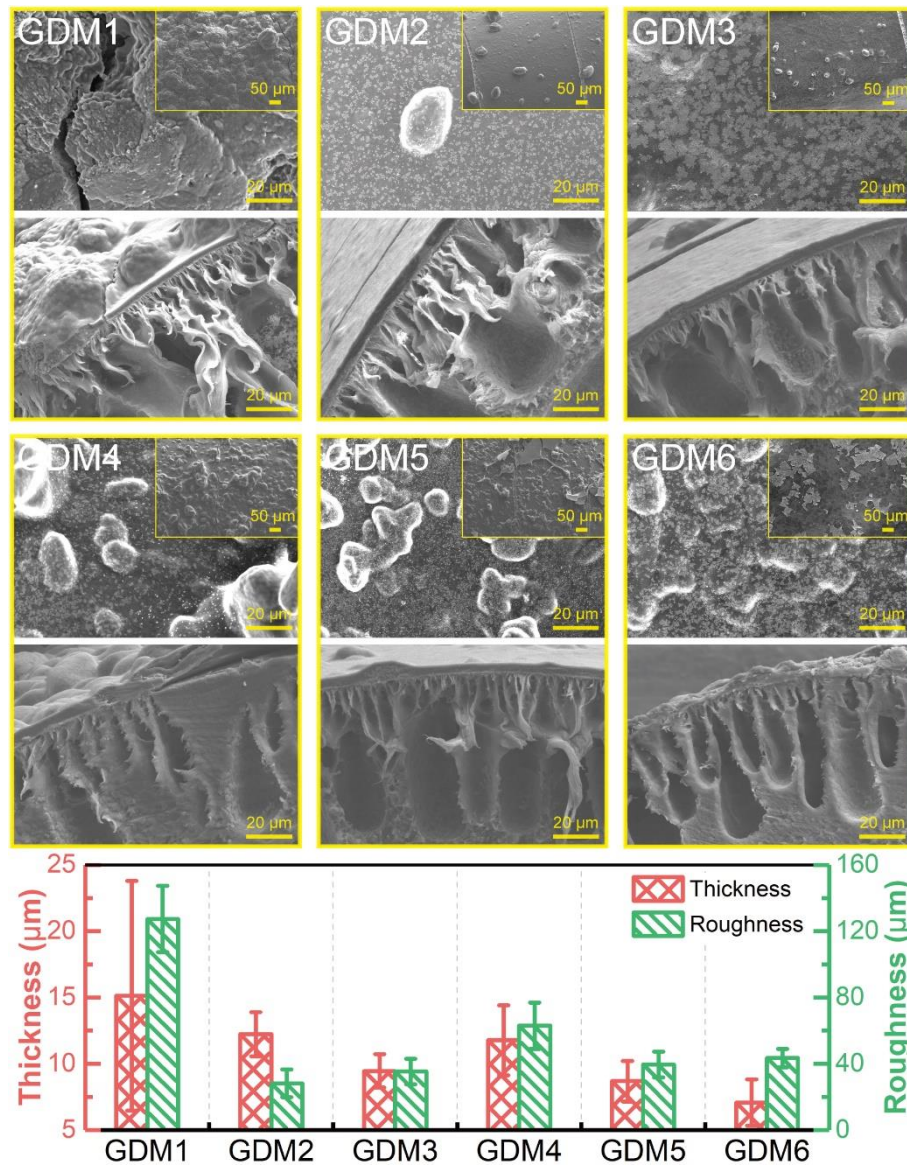
231 To summarize, pre-ozonation produced improved productivity in GDM filtration
232 systems, which in fact increased as a function of ozonation strength. Smaller and
233 more biodegradable organic compounds in the oxidized effluent would translate into a
234 somewhat facilitated passage of organics into the permeate stream, also exacerbated
235 by faster solubilization within the fouling layer. When adsorption of the oxidized
236 effluent was included as an intermediate pre-treatment step, a higher removal rate of
237 organics was consistently obtained compared to the treatment of the raw effluent
238 without pre-ozonation. As suggested by these results, different properties and a

239 different composition of the membrane fouling layers should be expected following
240 the different pre-treatment combinations, as fouling layers are a direct consequence of
241 feed stream characteristics and water flux values.

242 **3.2 Characteristics of membrane fouling layers**

243 [Fig. S4](#), [Fig. S5](#), and [Fig. 2](#) present surface and cross-sectional micrographs of
244 fouled membrane samples collected from the six GDM systems. A dense fouling layer
245 was always observed, also corroborated by the fact that the typical IR peaks of virgin
246 PVDF membrane disappeared in the FTIR spectra of fouled membranes ([Fig. S6c](#)).
247 The layer thickness and roughness were the largest for the control GDM unit, while
248 the distribution on the surface was very uneven. In addition, some pollutants were
249 also deposited within the membrane pores. Compared with GDM and GGDM, the
250 fouling layers of O₃-GDM systems were consistently thinner.

251 As summarized in [Fig. S6a](#), the membrane fouling resistance of GDM systems is
252 mainly reversible, with reversibility accounting for above 90% of the total resistance
253 value. The pure water contact angles of fouling layers ([Fig. S6b](#)) indicated that
254 pre-ozonation increased the hydrophilicity of the fouling layers by increasing the
255 hydrophilicity of pollutants, while simultaneously GAC adsorption decreased the
256 hydrophilicity of the fouling layers by absorbing hydrophilic pollutants.



257

258 Fig. 2 Surface (top; 500 × and 100 ×) and cross-sectional (bottom; 500 ×) micrographs

259 of the fouled membrane samples from the six GDM systems, as well as thickness and

260 roughness values measured for the membrane fouling layers. GDM1, GDM2, GDM3,

261 GDM4, GDM5, and GDM6 represent control GDM, GGDM, O₃²⁰-GGDM,

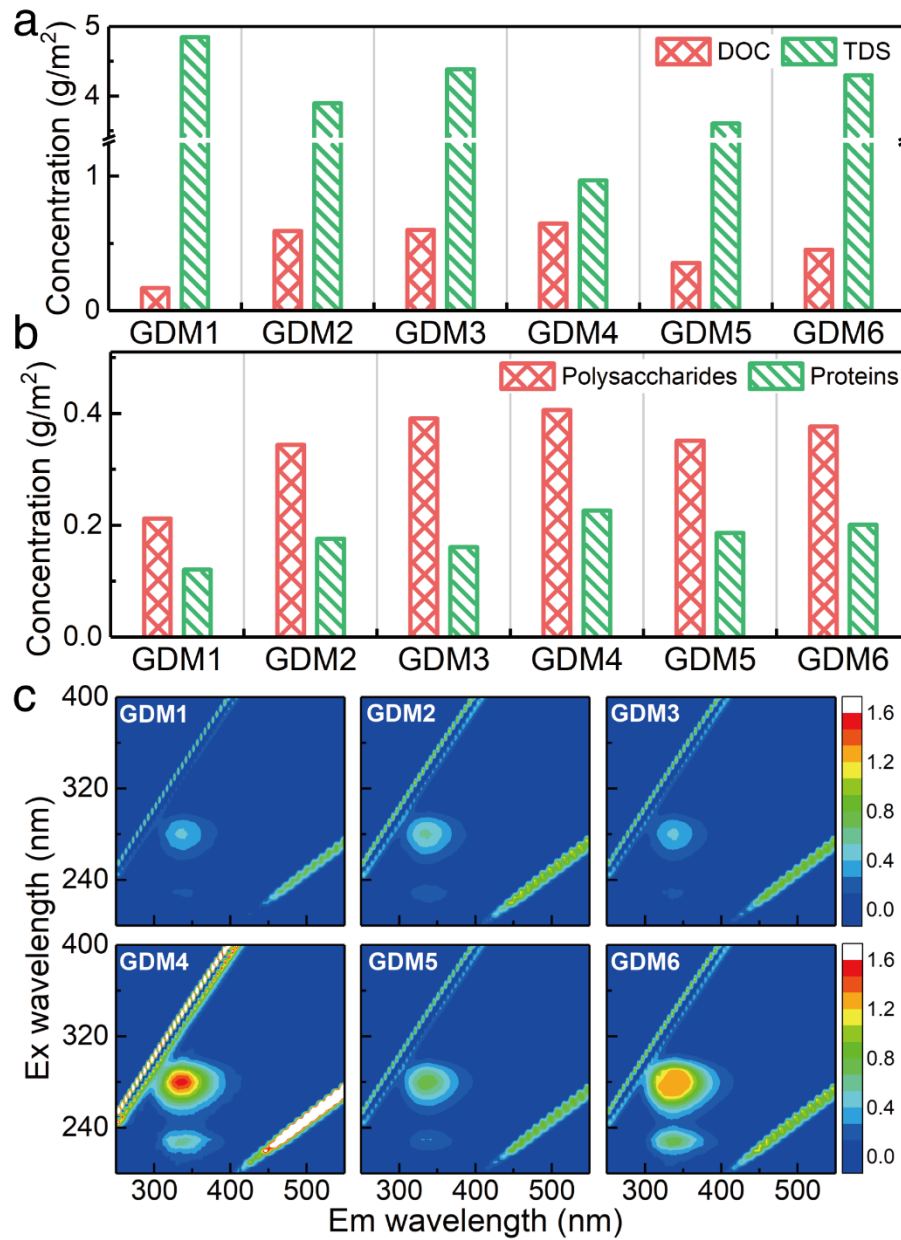
262 O₃⁴⁰-GDM, O₃⁴⁰-GGDM, and O₃⁸⁰-GGDM units, respectively.

263

264 The results presented in Fig. 3a suggest that the accumulation of overall organic

265 contaminants on the membrane of control GDM and O₃⁴⁰-GDM systems was the

266 lowest and the largest, respectively. This observation is corroborated by the amount of
267 EPS detected on the membranes and by the EEM analysis (Fig. 3b, c). The EPS
268 content of the fouling layer in the four O₃-GDM systems was higher than that
269 observed in GDM and GGDM units, and highest in the O₃⁴⁰-GDM unit. The same
270 conclusion can be also drawn for fluorescent organic compounds. In particular, these
271 compounds were distributed in region II (aromatic protein) and especially in region
272 IV (soluble microbial by-product-like matters), suggesting the important contribution
273 of transformation phenomena occurring within the fouling layer.



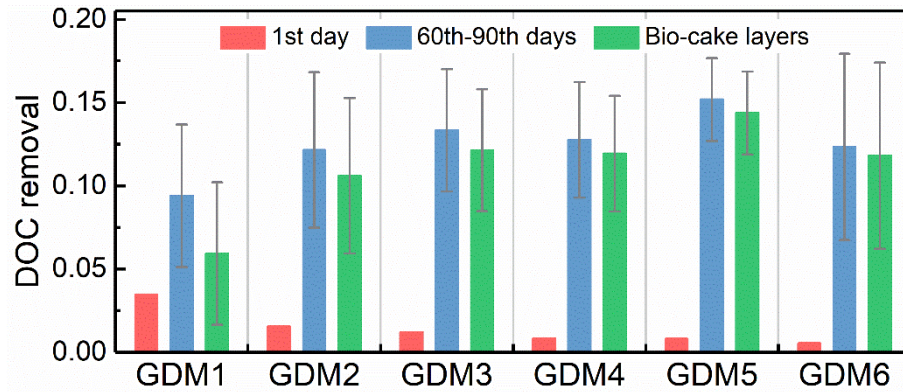
274

275 **Fig. 3** Concentration of (a) DOC and TDS, (b) EPS (includes polysaccharides and

276 proteins) in the fouling layers. (c) EEM spectra of compounds in the fouling layers.

277 GDM1, GDM2, GDM3, GDM4, GDM5, and GDM6 represent control GDM, GGDM,

278 O₃²⁰-GGDM, O₃⁴⁰-GDM, O₃⁴⁰-GGDM, and O₃⁸⁰-GGDM units, respectively.



279

280 Fig. 4 DOC removal of UF membrane of six GDM systems at 1st day and 60th-90th
 281 days of operation and DOC removal of fouling layers at 60th-90th days. GDM1,
 282 GDM2, GDM3, GDM4, GDM5, and GDM6 represent control GDM, GGDM,
 283 O_3^{20} -GGDM, O_3^{40} -GDM, O_3^{40} -GGDM, and O_3^{80} -GGDM, respectively.

284

285 The relative DOC removal rates of UF membranes can be obtained from the
 286 varying concentrations of DOC in the reactor and effluent at any time to understand
 287 the role of fouling layers as they form during operation (Fig. 4). The fouling layers
 288 perform three functions, namely., physical interception, adsorption, and
 289 biodegradation, which increase the contaminants removal in GDM systems (Tang et
 290 al., 2021d). Specifically, the DOC removal attributable to the fouling layer can be
 291 estimated by subtracting the DOC removal of the 1st day (no fouling layer present)
 292 from that observed during the stable flux stage (days 60-90) . The DOC removal of
 293 the fouling layer was 5.9% and 10.6% in control GDM and GGDM systems,
 294 respectively. This parameter was significantly higher in all units treating pre-ozonized
 295 streams. As mentioned above, the thickness of the fouling layer of GDM and GGDM

296 was thick and one would expect higher DOC removal by physical exclusion.
297 Therefore, the higher DOC removal assessed in the four O₃-GDM systems might be
298 attributed to the higher biodegradation function of the fouling layers. In our work, we
299 did not directly appraised the relative proportion of physical interception and
300 biodegradation mechanisms resulting in organic removal. However, previous research
301 indirectly determined the importance of these phenomena by adding biological
302 inhibitors, such as sodium azide (Tang et al., 2021d), with results consistent with the
303 present observations.

304 **3.3 Microbial diversity analysis**

305 The number of effective sequences, alpha diversity indexes, OUTs, and
306 rarefaction curves for microbial communities in the raw water and in the fouling layer
307 of the six GDM systems are presented in [Table 3](#) and [Fig.S7](#). The richness and
308 diversity of microbial communities in the raw water were higher than those on
309 membranes. The coverage values and rarefaction curves suggested the sequencing
310 depth were sufficient.

311 Principal component analysis (PCA) at OUT level ([Fig. S8](#)) provides information
312 on the affinity relationships of microbial community between the raw water and the
313 fouling layers in the six GDM systems, as well as among the six GDM systems. The
314 microbial community composition in the raw water was vastly different from that
315 observed in the samples from the six GDM systems, indicating new dominant
316 microorganisms had been formed in the filtration reactors. Also, pre-ozonation

317 seemed to have a large effect in the microbial community. The microbial community
 318 compositions from the four GDM systems treating pre-ozonized SGW as feed water
 319 were all similar, but different from the composition of the other two GDM systems
 320 This result also indicates that GAC had little effect on the microbial community.

321

322 **Table 3** Number of effective sequences, OTUs, alpha diversity indexes for microbial
 323 communities in the raw water and on the membrane of the six GDM systems.

Sample Name	Number of effective Sequences	OTUs at 97% identity	Shannon	Chao	Coverage
Raw water	36178	316	3.83	334.6	0.9988
GDM1	36064	115	2.50	119.2	0.9996
GDM2	30672	113	2.68	121.3	0.9994
GDM3	28903	88	2.52	107.4	0.9993
GDM4	29351	62	2.75	66.2	0.9997
GDM5	29713	92	2.93	105.0	0.9994
GDM6	24814	81	3.01	84.0	0.9997

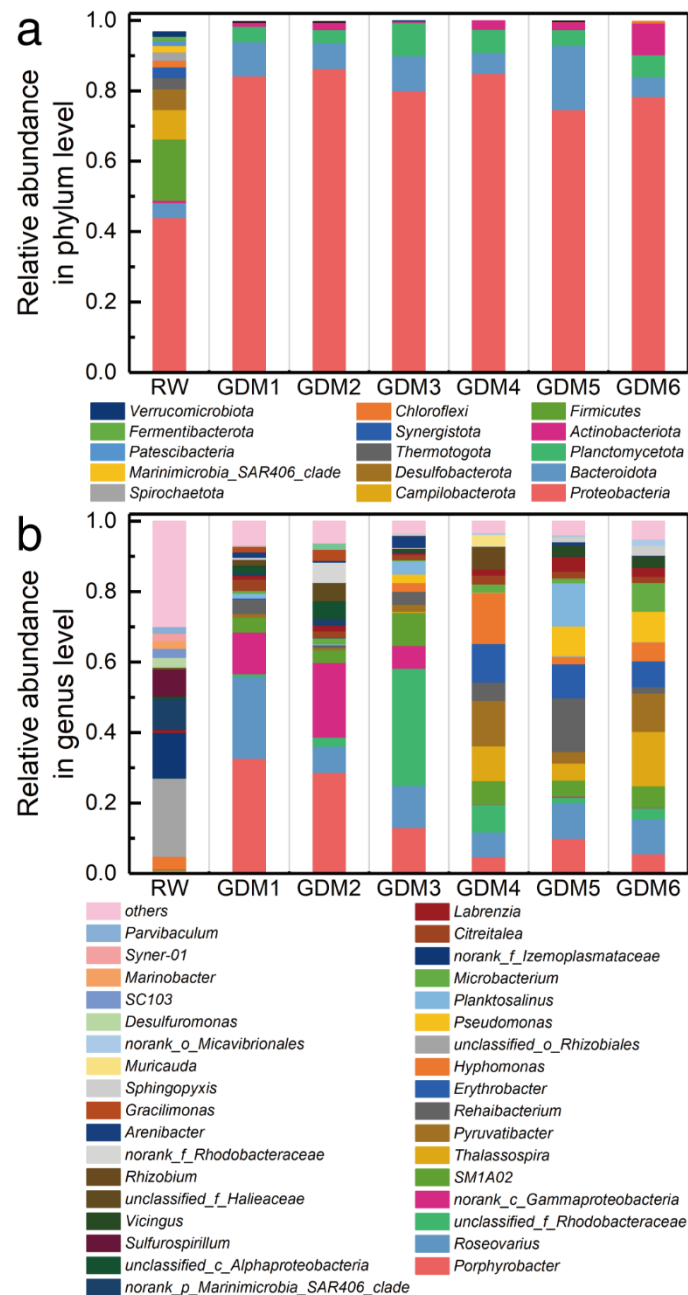
324

325 **Fig. 5a** and **Fig. 5b** show the microbial community composition at the phylum
 326 and genus level, respectively. *Proteobacteria* (44.1%), *Firmicutes* (17.5%),
 327 *Campilobacterota* (8.4%), *Desulfobacterota* (5.9%), and *Bacteroidota* (4.2%) were
 328 the major phyla in the raw water, comprising 80.1% of bacteria. After operation,
 329 *Proteobacteria* (74.8%-86.5%) and *Bacteroidota* (5.6%-18.2%) became the absolute
 330 dominant microbial phyla in GDM reactors. The major genera in the raw water were
 331 *unclassified_o_Rhizobiales*, *norank_f_Izemoplasmataceae*, *Parvibaculum*,

332 *Sulfurospirillum*, and *Desulfuromonas*. A large amount of relatively low abundance
333 microorganisms (<0.5%) was enriched in GDM systems, like *Porphyrobacter*
334 (4.8-32.8%), *Roseovarius* (7.0-23.2%), *unclassified_f_Rhodobacteraceae* (0.8-33.3%),
335 *SMIA02* (3.6%-9.4%), *Pyruvatibacter* (0.6%-13.0%) and *Rehaibacterium*
336 (0.5-15.2%). Some research showed that members of *Porphyrobacter* can degrade
337 organics, such as polycyclic aromatic hydrocarbons (Balázs et al., 2020; Fan et al.,
338 2016). *Roseovarius*, as an iodine oxidation bacterium, can promote the formation of
339 large amounts of iodinated organic compounds (Almaraz et al., 2020).
340 *Rhodobacteraceae* were widely reported in various environments with ability of
341 degrading organic matter and removing nitrogen (Chen et al., 2021; Ma et al., 2020).
342 Some works proved that *Pyruvatibacter* as a halophilic bacterium can degrade
343 acetoacetic acid and pyruvate (Wang et al., 2016). *Rehaibacterium* was reported as a
344 thermotolerant, halophilic, and strictly aerobic bacterium with the function of
345 degrading some organic compounds (Yu et al., 2013).

346 In this work, O₃-GDM systems had their own characteristic microorganisms.
347 Specifically, *Porphyrobacter* and *norank_c_Gammaproteobacteria*, were enriched in
348 the two GDM systems treating non-ozonized SGW as feed water. *Thalassospira*
349 (5.0-15.5%), *Pyruvatibacter* (3.2-13.0%), and *Erythrobacter* (7.2-10.9%) were
350 enriched in three of the O₃-GDM systems. It was reported that some species of
351 *Thalassospira* can degrade quaternary ammonium compounds, which are often used
352 as biocides in SGW (Acharya et al., 2020). *Pyruvatibacter* as an aerobic marine

353 bacterium can degrade some organics, such as pyruvate (Wang et al., 2016). As
 354 aerobic phototrophs, *Erythrobacter* often exist in organic-rich environments, and can
 355 degrade PAHs, one of the main organic pollutants in SGW (Butkovskiy et al., 2017;
 356 Kahla et al., 2021).



357
 358 **Fig. 5** Bacterial community compositions at (a) the phylum (> 1%) and (b) the genus
 359 level (> 1.5%) in raw water and on the membrane of the six GDM systems. GDM1,

360 GDM2, GDM3, GDM4, GDM5, and GDM6 represent control GDM, GGDM,
361 O_3^{20} -GGDM, O_3^{40} -GDM, O_3^{40} -GGDM, and O_3^{80} -GGDM units, respectively.

362

363 **3.4 Summary on mechanisms and effect of pre-ozonation on GDM systems and** 364 **desalination**

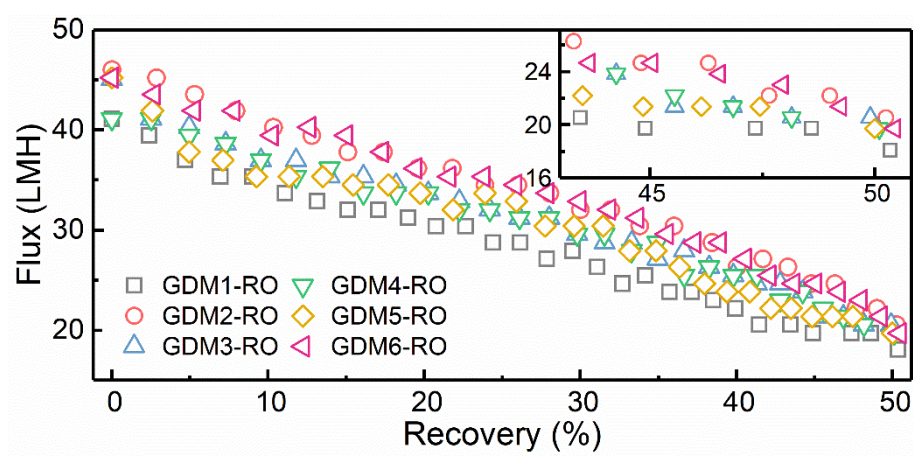
365 The rapid decline of flux in GDM system should be attributed to the blocking of
366 membrane pores by the rapid formation of dense fouling layer (Fig. 1 and Fig. 2).
367 Pre-ozonation significantly increased the initial flux (245%) but deteriorated the
368 quality of effluent water in terms of DOC concentration (-14%) (Fig. 1). These results
369 are mainly attributed to the conversion of macromolecular organics to low fractions
370 by pre-ozonation (Fig. 1 and Fig. 4). EPS played an important role in flux
371 development of GDM, and a large number of studies found negative correlation
372 between EPS content and stable flux (Pronk et al., 2019; Tang et al., 2021d). However,
373 some contradictory results were observed in this study. O_3 -GDM system had higher
374 EPS concentration compared to GDM (Fig. 3), while the stable flux of O_3 -GDM
375 system was 3.7 times of GDM. This observation suggests that there were other factors
376 that played roles in stabilizing the flux. Compared with GDM, it was observed that the
377 thickness of the fouling layer of O_3 -GDM system was thinner, the hydrophilicity of
378 the fouling layer was higher, and biodegradation ability of the fouling layer was
379 enhanced (Fig. 2, Fig. S6, and Fig. 4). All these factors might play a positive function
380 in the improvement of stable flux. However, we hypothesize that the reduction of

381 organics molecular size may be the main result of pre-ozonation that increased the
382 stable flux.

383 Compared with GDM, GGDM had higher stable flux (637%), likely because
384 GAC adsorption reduced the concentration of organic matters blocking membrane
385 pores. For GGDM systems, pre-ozonation also markedly increased the flux (198%) in
386 the first month of operation. Pre-ozonation improved the stable flux by reducing
387 organics molecular size and GAC adsorption improved the stable flux by reducing the
388 concentration of organic matters blocking membrane pores, also simultaneously
389 improving the quality of the effluent.

390 The permeate of the six GDM systems was collected and fed individually to the
391 RO system to study the effect of pretreatment on RO performance. The RO flux was
392 higher when treating effluents that were previously ozonized, despite the fact the the
393 DOC level in these streams was not necessarily lower than that from the control
394 system ([Fig. 6](#)). Considering that the RO unit was operating in dead-end mode, the
395 observed increase (9%) can be considered significant (Chang et al., 2019a). Some
396 research found that pre-ozonation reduced RO membrane fouling by improving the
397 hydrophilicity of foulants and weakening the adhesion forces between foulants and
398 the membrane and among foulants (Yin et al., 2020a,b). Furthermore, the use of GAC
399 significantly increased the flux of GDM-RO (13.6%) and slightly improve the flux of
400 O₃-GDM-RO. GAC adsorption may further reduce RO membrane fouling by
401 decreasing the overall content of organic foulants (Monnot et al., 2017). [Table S1](#)

402 presents the effluent quality of six GDM-RO systems and indicates that within the
 403 range of errors, the water quality of the six systems was almost the same. In general,
 404 O₃-GDM outperformed GDM in terms of productivity.



405

406 **Fig. 6** Effect of pretreatments on the RO desalination performance. GDM1, GDM2,
 407 GDM3, GDM4, GDM5, and GDM6 represent control GDM, GGDM, O₃²⁰-GGDM,
 408 O₃⁴⁰-GDM, O₃⁴⁰-GGDM, and O₃⁸⁰-GGDM units, respectively.

409

410 **4. Conclusions**

411 Pre-ozonation was investigated in combination with GAC adsorption and with
 412 GDM system to treat SGW. Pre-ozonation changed the properties and molecular
 413 weight of organic compounds. Macromolecular organics are oxidized by ozonation to
 414 low fractions organics, which have a lower fouling tendency, can more easily pass
 415 through the membrane pores, and can be more readily biodegraded the the
 416 microorganisms in the fouling layers. At the same time, the decrease of the molecular
 417 weight of organic matter also led to the deterioration of the effluent quality of
 418 O₃-GDM in terms of organic content. The higher concentration of organic compounds

419 in the feed solution and the laerger amount of EPS in the fouling layers of O₃-GDM
420 systems may be the reason why the stable flux of the systems treating ozonized
421 effluents without adsorption was lower than that of systems including GAC. A large
422 number of microorganisms with the ability to degrade organics and of denitrification
423 were generally enriched in the membrane fouling layer. The O₃-GDM systems had
424 distinct core microorganisms that may help degrade characteristic organic compounds
425 in SGW, such as quaternary ammonium compounds and PAHs. The contribution of
426 microorganisms in the degradation of organic matter needs further investigation.

427 **Supporting Information**

428 The Supporting Information is available free of charge on the website.

429 **Acknowledgments**

430 This work was supported by the National Natural Science Foundation of China
431 (52070134, 51678377), Xinglin Environment Project (2020CDYB-H02), and Sichuan
432 University and Yibin City People's Government strategic cooperation project
433 (2019CDYB-25). Thanks to the SEM measurement of the Institute of New Energy
434 and Low-Carbon Technology, Sichuan University.

435 **References**

- 436 Acharya, S.M., Chakraborty, R. and Tringe, S.G. 2020. Emerging Trends in
437 Biological Treatment of Wastewater From Unconventional Oil and Gas Extraction.
438 *Front. Microbiol.* 11(2203). 10.3389/fmicb.2020.569019
- 439 Almaraz, N., Regnery, J., Vanzin, G.F., Riley, S.M., Ahoor, D.C. and Cath, T.Y.
440 2020. Emergence and fate of volatile iodinated organic compounds during biological
441 treatment of oil and gas produced water. *Sci. Total Environ.* 699, 134202.
442 <https://doi.org/10.1016/j.scitotenv.2019.134202>
- 443 Balázs, H.E., Schmid, C.A.O., Podar, D., Hufnagel, G., Radl, V. and Schröder, P.
444 2020. Development of microbial communities in organochlorine pesticide
445 contaminated soil: A post-reclamation perspective. *Appl. Soil Ecol.* 150, 103467.
446 <https://doi.org/10.1016/j.apsoil.2019.103467>
- 447 Butkovskiy, A., Bruning, H., Kools, S.A.E., Rijnaarts, H.H.M. and Van Wezel,
448 A.P. 2017. Organic pollutants in shale gas flowback and produced waters: Identification,
449 potential ecological impact, and implications for treatment strategies. *Environ. Sci.*
450 *Technol.* 51(9), 4740-4754. <https://doi.org/10.1021/acs.est.6b05640>
- 451 Chang, H., Liu, B., Wang, H., Zhang, S.Y., Chen, S., Tiraferri, A. and Tang, Y.Q.
452 2019a. Evaluating the performance of gravity-driven membrane filtration as
453 desalination pretreatment of shale gas flowback and produced water. *J. Membr. Sci.*
454 587, 117187. <https://doi.org/10.1016/j.memsci.2019.117187>
- 455 Chang, H., Liu, B., Yang, B., Yang, X., Guo, C., He, Q., Liang, S., Chen, S. and
456 Yang, P. 2019b. An integrated coagulation-ultrafiltration-nanofiltration process for
457 internal reuse of shale gas flowback and produced water. *Sep. Purif. Technol.* 211,
458 310-321. <https://doi.org/10.1016/j.seppur.2018.09.081>
- 459 Chen, Z., Chang, Z., Qiao, L., Wang, J., Yang, L., Liu, Y., Song, X. and Li, J. 2021.
460 Nitrogen removal performance and microbial diversity of bioreactor packed with
461 cellulosic carriers in recirculating aquaculture system. *International Biodeterioration &*
462 *Biodegradation* 157, 105157. <https://doi.org/10.1016/j.ibiod.2020.105157>
- 463 Ding, A., Liang, H., Li, G., Derlon, N., Szivak, I., Morgenroth, E. and Pronk, W.
464 2016. Impact of aeration shear stress on permeate flux and fouling layer properties in a
465 low pressure membrane bioreactor for the treatment of grey water. *J. Membr. Sci.* 510,
466 382-390. <https://doi.org/10.1016/j.memsci.2016.03.025>
- 467 Fan, M., Lin, Y., Huo, H., Liu, Y., Zhao, L., Wang, E., Chen, W. and Wei, G. 2016.
468 Microbial communities in riparian soils of a settling pond for mine drainage treatment.
469 *Water Res.* 96, 198-207. <https://doi.org/10.1016/j.watres.2016.03.061>
- 470 Guo, C., Chang, H., Liu, B., He, Q., Xiong, B., Kumar, M. and Zydney, A.L. 2018.
471 A combined ultrafiltration–reverse osmosis process for external reuse of Weiyuan shale
472 gas flowback and produced water. *Environ. Sci. Water Res. Technol.* 4(7), 942-955.
473 <https://doi.org/10.1039/C8EW00036K>
- 474 Kahla, O., Melliti Ben Garali, S., Karray, F., Ben Abdallah, M., Kallel, N., Mhiri,
475 N., Zaghden, H., Barhoumi, B., Pringault, O., Quéméneur, M., Tedetti, M., Sayadi, S.

476 and Sakka Hlaili, A. 2021. Efficiency of benthic diatom-associated bacteria in the
477 removal of benzo(a)pyrene and fluoranthene. *Sci. Total Environ.* 751, 141399.
478 <https://doi.org/10.1016/j.scitotenv.2020.141399>

479 Kondash, A. and Vengosh, A. 2015. Water footprint of hydraulic fracturing.
480 *Environ. Sci. Technol. Lett.* 2, 276–280. 10.1021/acs.estlett.5b00211

481 Lee, S., Badoux, G.O., Wu, B. and Chong, T.H. 2021. Enhancing performance of
482 biocarriers facilitated gravity-driven membrane (GDM) reactor for decentralized
483 wastewater treatment: Effect of internal recirculation and membrane packing density.
484 *Sci. Total Environ.* 762, 144104. <https://doi.org/10.1016/j.scitotenv.2020.144104>

485 Liu, P., Ren, Y., Ma, W., Ma, J. and Du, Y. 2018. Degradation of shale gas
486 produced water by magnetic porous MFe₂O₄ (M = Cu, Ni, Co and Zn) heterogeneous
487 catalyzed ozone. *Chem. Eng. J.* 345, 98-106. <https://doi.org/10.1016/j.cej.2018.03.145>

488 Ma, K., Li, X., Bao, L., Li, X. and Cui, Y. 2020. The performance and bacterial
489 community shifts in an anaerobic-aerobic process treating purified terephthalic acid
490 wastewater under influent composition variations and ambient temperatures. *J. Clean.*
491 *Prod.* 276, 124190. <https://doi.org/10.1016/j.jclepro.2020.124190>

492 Miller, D.J., Huang, X., Li, H., Kasemset, S., Lee, A., Agnihotri, D., Hayes, T.,
493 Paul, D.R. and Freeman, B.D. 2013. Fouling-resistant membranes for the treatment of
494 flowback water from hydraulic shale fracturing: A pilot study. *J. Membr. Sci.* 437,
495 265-275. <https://doi.org/10.1016/j.memsci.2013.03.019>

496 Monnot, M., Nguyễn, H.T.K., Laborie, S. and Cabassud, C. 2017. Seawater
497 reverse osmosis desalination plant at community-scale: Role of an innovative
498 pretreatment on process performances and intensification. *Chemical Engineering and*
499 *Processing: Process Intensification* 113, 42-55.
500 <https://doi.org/10.1016/j.cep.2016.09.020>

501 Pronk, W., Ding, A., Morgenroth, E., Derlon, N., Desmond, P., Burkhardt, M., Wu,
502 B. and Fane, A.G. 2019. Gravity-driven membrane filtration for water and wastewater
503 treatment: A review. *Water Res.* 149, 553-565.
504 <https://doi.org/10.1016/j.watres.2018.11.062>

505 Sathya, U., Keerthi, Nithya, M. and Balasubramanian, N. 2019. Evaluation of
506 advanced oxidation processes (AOPs) integrated membrane bioreactor (MBR) for the
507 real textile wastewater treatment. *J. Environ. Manag.* 246, 768-775.
508 <https://doi.org/10.1016/j.jenvman.2019.06.039>

509 Shang, W., Tiraferri, A., He, Q., Li, N., Chang, H., Liu, C. and Liu, B. 2019. Reuse
510 of shale gas flowback and produced water: Effects of coagulation and adsorption on
511 ultrafiltration, reverse osmosis combined process. *Sci. Total Environ.* 689, 47-56.
512 <https://doi.org/10.1016/j.scitotenv.2019.06.365>

513 Tang, P., Li, J., Li, T., Tian, L., Sun, Y., Xie, W., He, Q., Chang, H., Tiraferri, A.
514 and Liu, B. 2021a. Efficient integrated module of gravity driven membrane filtration,
515 solar aeration and GAC adsorption for pretreatment of shale gas wastewater. *J. Hazard.*
516 *Mater.* 405, 124166. <https://doi.org/10.1016/j.jhazmat.2020.124166>

517 Tang, P., Liu, B., Zhang, Y., Chang, H., Zhou, P., Feng, M. and Sharma, V.K. 2020.

518 Sustainable reuse of shale gas wastewater by pre-ozonation with ultrafiltration-reverse
519 osmosis. Chem. Eng. J. 392, 123743. <https://doi.org/10.1016/j.cej.2019.123743>
520 Tang, P., Xie, W., Tiraferri, A., Zhang, Y., Zhu, J., Li, J., Lin, D., Crittenden, J.C.
521 and Liu, B. 2021b. Organics removal from shale gas wastewater by pre-oxidation
522 combined with biologically active filtration. Water Res. 196, 117041.
523 <https://doi.org/10.1016/j.watres.2021.117041>
524 Tang, X., Pronk, W., Traber, J., Liang, H., Li, G. and Morgenroth, E. 2021c.
525 Integrating granular activated carbon (GAC) to gravity-driven membrane (GDM) to
526 improve its flux stabilization: Respective roles of adsorption and biodegradation by
527 GAC. Sci. Total Environ. 768, 144758. <https://doi.org/10.1016/j.scitotenv.2020.144758>
528 Tang, X., Zhu, X., Huang, K., Wang, J., Guo, Y., Xie, B., Li, G. and Liang, H.
529 2021d. Can ultrafiltration singly treat the iron- and manganese-containing groundwater?
530 J. Hazard. Mater. 409, 124983. <https://doi.org/10.1016/j.jhazmat.2020.124983>
531 Tong, T., Carlson, K.H., Robbins, C.A., Zhang, Z. and Du, X. 2019.
532 Membrane-based treatment of shale oil and gas wastewater: The current state of
533 knowledge. Front. Env. Sci. Eng. 13(4), 63.
534 <https://doi.org/10.1016/j.watres.2020.115694>
535 Wang, G., Tang, M., Wu, H., Dai, S., Li, T., Chen, C., He, H., Fan, J., Xiang, W.
536 and Li, X. 2016. *Pyruvatibacter mobilis* gen. nov., sp. nov., a marine bacterium from the
537 culture broth of *Picochlorum* sp. 122. 66(1), 184-188.
538 <https://doi.org/10.1099/ijsem.0.000692>
539 Wang, H., Park, M., Liang, H., Wu, S., Lopez, I.J., Ji, W., Li, G. and Snyder, S.A.
540 2017. Reducing ultrafiltration membrane fouling during potable water reuse using
541 pre-ozonation. Water Res. 125, 42-51. 10.1016/j.watres.2017.08.030
542 Yin, Z., Wen, T., Li, Y., Li, A. and Long, C. 2020a. Alleviating reverse osmosis
543 membrane fouling caused by biopolymers using pre-ozonation. J. Membr. Sci. 595,
544 117546. <https://doi.org/10.1016/j.memsci.2019.117546>
545 Yin, Z., Wen, T., Li, Y., Li, A. and Long, C. 2020b. Pre-ozonation for the
546 mitigation of reverse osmosis (RO) membrane fouling by biopolymer: The roles of
547 Ca^{2+} and Mg^{2+} . Water Res. 171, 115437. <https://doi.org/10.1016/j.watres.2019.115437>
548 Yu, T.-T., Yao, J.-C., Yin, Y.-R., Dong, L., Liu, R.-F., Ming, H., Zhou, E.-M. and
549 Li, W.-J. 2013. *Rehaibacterium terrae* gen. nova, sp nov isolated from a geothermally
550 heated soil sample. Int. J. Syst. Evol. Micr. 63, 4058-4063. 10.1099/ijss.0.049973-0
551 Zhang, K., Zhang, Z.-h., Wang, H., Wang, X.-m., Zhang, X.-h. and Xie, Y.F. 2020.
552 Synergistic effects of combining ozonation, ceramic membrane filtration and
553 biologically active carbon filtration for wastewater reclamation. J. Hazard. Mater. 382,
554 121091. <https://doi.org/10.1016/j.jhazmat.2019.121091>
555